Robust Unit Commitment with Large-Scale Battery Storage

Kristina Jurković, *Student Member, IEEE*, Hrvoje Pandžić, *Member, IEEE*, Igor Kuzle, *Senior Member, IEEE*

***Abstract*—As the renewable energy levels are constantly increasing, scheduling of generating units in the day ahead stage is becoming more challenging for system operators. Energy storage is emerging as an attractive solution for dealing with uncertainty and variability of renewable generation. Specifically, large-scale battery storage units are gaining popularity due to their modularity, fast response and ongoing cost reduction.**

In this paper we model a two-stage adaptive robust unit commitment model with large-scale energy storage. The objective is to minimize the operating costs of thermal generators under the worst wind power output scenario. The over-protection is addressed using a parameter that controls the conservatism of the model. This control parameter can be extended to cover the uncertainty more realistically using multiple bands as the time horizon progresses.

The proposed model is tested on an updated IEEE RTS-96 system. Different levels of protecting the system against uncertainty are evaluated and the role of energy storage is analyzed.

***Index Terms*—Robust unit commitment, energy storage, wind uncertainty, multiband uncertainty, Benders' decomposition**

I. Introduction

A. Motivation

Increasing levels of renewable energy in modern power systems pose a challenge for system operators to make economic and efficient, yet reliable and adequate day-ahead unit commitment (UC) decisions. There are different ways to manage the risk the renewables bring to the power systems. The most common is to define different types of reserves and their levels [1]–[3]. With high volatility of the renewables, especially wind energy, this kind of system protection is not economically efficient.

An explicit way to considering uncertainty of renewables' output is to use scenarios of different probabilities [4]–[6]. These scenarios are usually derived from historical data and/or weather forecasts. Such model yields acceptable system cost, but in order to achieve robustness it may require a large number of scenarios which affects the computational tractability of the model.

In order to avoid long computational times of the scenario-based stochastic model, interval and robust models were derived. These models do not consider probability distribution. Instead, their uncertainty set considers only the bounds of uncertainty, resulting in higher computational efficiency. However, both interval and robust UC models result in less efficient day-ahead schedules [7].

Interval UC minimizes the cost of the most likely scenario while ensuring the feasibility of the schedule within the entire uncertainty set. This is achieved by imposing feasibility along the upper and lower bounds, as well as imposing ramp requirements between the bounds in between each two consecutive time periods. Robust UC also uses uncertainty set instead of scenarios, but the objective function is to minimize the cost of the worst case wind scenario [7]–[9].

The motivation for this paper lies in the increasing popularity of unconventional large-scale storage, more specifically large-scale batteries. According to the DoE's Global Energy Storage Database, currently there is over 1.7 GW of operational and 660 MW of contracted battery storage capacity worldwide [10]. This indicates that, although the capacity of unconventional large-scale battery storage is still low, its growth is rapid. This is mostly the result of energy policies that support the installation of storage units in order to enable higher integration of renewable sources [11]. Therefore, the goal of this paper is to integrate large-scale battery storage with robust UC model in order to assess its impact and role.

B. Literature Review

The authors in [12] propose a two-stage adaptive security-constrained robust UC dealing with uncertain nodal net injections. The uncertainty is described using a deterministic set and the level of robustness is controlled using the budget of uncertainty. This budget of uncertainty controls the number of nodal net injections that can deviate from their nominal values. The solutions of the model are robust against all possible realizations of the modeled uncertainty. Since the subproblem is a bilinear optimization problem, it is solved by outer approximation technique which guarantees only a local optimum.

A model that captures the uncertainty in a polyhedral set and incorporates demand response is presented in [13]. The authors avoid bilinearity of the subproblem by converting it into a mixed integer linear problem (MILP) and solve the robust UC by employing both Benders decomposition type of algorithm, as well as column and constraint generation algorithm (C&CG) [14].

A two-dimensional uncertainty set allowing the uncertainty correlations among different buses and time periods is introduced in [15]. The problem is solved using an exact and a bilinear heuristic separation approach within a Benders' decomposition frame.

In paper [16], the authors formulate robust UC that tackles wind power uncertainty with pumped storage hydro power plants. The authors assume that the uncertain parameter, wind generation, is within the interval constructed based on historical data with the forecasted value being the mean value

978-1-5386-2212-4/17/$31.00 ©2017 IEEE

of the interval. The budget of uncertainty controls the number of hours in which the wind farm can deviate.

We present a robust unit commitment with large scale energy storage with increasingly higher protection levels.

II. Formulation

A. Notation

1) Sets:

b Index to the piecewise linear segments of each generating unit's offer curve, from 1 to B.
i Index to the generating units, from 1 to I.
j Index to the start-up cost of generating units, from 1 to J.
l Index to the transmission lines, from 1 to L.
m Index to the storages, from 1 to M.
s Index to the buses, from 1 to S.
t Index to the hours, from 1 to T.
w Index to the wind farms, from 1 to W.

2) Binary variables:

$q_{t,i,j}$ Start-up cost curve segment identification.
$x_{t,i}$ Generator status, 1 if online.
$y_{t,i}$ Generator start-up indicator, 1 if started.
$z_{t,i}$ Generator shut down indicator, 1 if shut down.

3) Continuous variables:

$c_{t,w}$ Curtailed wind by wind farm w during hour t (MWh).
$E_{t,m}$ State of charge of storage m during hour t (MWh).
$g_{t,i,b}$ Power output on segment b of generator i during hour t (MWh).
$LS_{t,s}$ Load shedding during hour t at bus s (MWh).
$PC_{t,m}$ Power charged by storage m during hour t (MW).
$PD_{t,m}$ Power discharged by storage m during hour t (MW).
$f_{t,l}$ Power flow through line $s-m$ during hour t (MWh).
$r_{t,w}$ Wind deviation of wind farm w during hour t (MWh).
$r^{+}_{t,w}$ Postive wind deviation of wind farm w during hour t (MWh).
$r^{-}_{t,w}$ Negative wind deviation of wind farm w during hour t (MWh).
$su_{t,i}$ Start-up cost of generator i during hour t (\$/h).
$\theta_{t,s}$ Voltage angle of bus s during hour t (rad).

4) Parameters:

A_i Fixed cost of generator i (\$/MWh).
B_l Susceptance of line l (S).
cs_m Storage m operating cost (\$).
$D_{t,s}$ Demand during hour t on bus s (MWh).
$E^{\max}_m$ Maximum state of charge of storage m (MWh).
$E^{\min}_m$ Minimum state of charge of storage m (MWh).
E^{0}_m Initial state of charge of storage m (MWh).
η^{c}_m Charging efficiency of storage m.
η^{d}_m Discharging efficiency of storage m.
$G^{\max}_{i,b}$ Maximum production of generator i on segment b (MWh).
$G^{\min}_i$ Minimum production of generator i (MWh).
Γ Budget of uncertainty.
$k_{i,b}$ Cost curve segment b of generator i (\$/MWh).
$\overline{f}_l$ Transmission capacity of line l (MWh).
$PC^{\max}_m$ Maximum charging power of storage m (MW).
$PD^{\max}_m$ Maximum discharging power of storage m (MW).
RD_i Ramp down limit of generator i (MW/h).
RU_i Ramp up limit of generator i (MW/h).
$SUC_{i,j}$ Start-up cost of generator i on segment j (\$).
$VoLL$ Value of lost load (\$).
$wg_{t,w}$ Forecasted wind production by wind farm w during hour t (MWh).

B. Model Formulation

The optimization problem that aims to minimize total system operating cost under the worst wind realization is formulated as follows:

$$\begin{aligned}\max_{r_{t,w}} \quad & \min_{\substack{q_{t,i,j},x_{t,i},y_{t,i},z_{t,i},\\ su_{t,i},\\ g_{t,i,b},LS_{t,s},c_{t,w},\\ f_{t,l},\theta_{t,s}}} \sum_{t=1}^{T}\sum_{i=1}^{I}[su_{t,i}+A_i\cdot x_{t,i}\,]+\\ &+\sum_{t=1}^{T}\sum_{i=1}^{I}\sum_{b=1}^{B}k_{ib}\cdot g_{t,i,b}+\sum_{t=1}^{T}\sum_{s=1}^{S}VoLL\cdot LS_{t,s}+\\ &+\sum_{t=1}^{T}\sum_{m=1}^{M}[cs_m\cdot(PD_{t,m}+PC_{t,m})]\end{aligned} \tag{1}$$

subject to:

$$y_{t,i}-z_{t,i}=x_{t,i}-x_{t-1,i},\quad \forall t\le T, i\le I \tag{2}$$

$$y_{t,i}+z_{t,i}\le 1,\quad \forall t\le T, i\le I \tag{3}$$

$$x_{t,i}=x_{t_0,i},\quad \forall t\in\left[0,\overline{L}_i+\underline{L}_i\right], i\le I \tag{4}$$

$$\sum_{r=t-UT_i+1}^{t} y_{r,i}\le x_{t,i},\quad \forall t\in\left[\overline{L}_i,T\right], i\le I \tag{5}$$

$$\sum_{r=t-DT_i+1}^{t} z_{r,i}\le 1-x_{t,i},\quad \forall t\in\left[\underline{L}_i,T\right], i\le I \tag{6}$$

$$q_{t,i,j}\le\sum_{r=\underline{T}_{i,j}}^{\overline{T}_{i,j}} z_{t-r,i},\quad \forall t\le T, i\le I, j\le J \tag{7}$$

$$\sum_{j\in\Omega^{\mathrm{J}}} q_{t,i,j}=y_{t,i},\quad \forall t\le T, i\le I \tag{8}$$

$$su_{t,i}=\sum_{j\in\Omega^{\mathrm{J}}} SUC_{i,j}\cdot q_{t,i,j},\quad \forall t\le T, i\le I \tag{9}$$

$$\sum_{b=1}^{B} g_{t,i,b}\ge G^{\min}_i\cdot x_{t,i}\quad \forall t\le T, i\le I \tag{10}$$

$$g_{t,i,b}\le G^{\max}_{i,b}\cdot x_{t,i}\quad \forall t\le T, i\le I, b\le B \tag{11}$$

$$\sum_{b=1}^{B} g_{t-1,i,b}-\sum_{b=1}^{B} g_{t,i,b}\le \mathrm{RD}_i\quad \forall t\le T, i\le I \tag{12}$$

$$\sum_{b=1}^{B} g_{t,i,b}-\sum_{b=1}^{B} g_{t-1,i,b}\le \mathrm{RU}_i\quad \forall t\le T, i\le I \tag{13}$$

$$0\le PD_{t,m}\le PD^{\max}_m\quad \forall t\le T, m\le M \tag{14}$$

$$0\le PC_{t,m}(t)\le PC^{\max}_m\quad \forall t\le T, m\le M \tag{15}$$

978-1-5386-2212-4/17/$31.00 ©2017 IEEE

$$E_{t,m} = E_{t-1,m} + \eta_m^C \cdot PC_{t,m} - \frac{1}{\eta_m^D} \cdot PD_{t,m} \quad \forall t \le T, m \le M \tag{16}$$

$$E_m^{\min} \le E_{t,m} \le E_m^{\max} \quad \forall t \le T, m \le M \tag{17}$$

$$E_{T,m} = E_m^0 \quad \forall t = T, m \le M \tag{18}$$

$$\sum_{i=1|i\in S}^{I} \sum_{b=1}^{B} g_{t,i,b} - \sum_{w=1|w\in S}^{W} c_{t,w} - \sum_{l=1|l\in S}^{L} f_{t,l} + LS_{t,s} + \sum_{m=1|m\in S}^{M} (PD_{t,m} - PC_{t,m}) = D_{t,s} - \sum_{w=1|w\in S}^{W} (wg_{t,w} + r_{t,w}) \quad \forall t \le T, s \le S \tag{19}$$

$$f_{t,l} - B_l \cdot \sum_{s=1|s\in L}^{S} \theta_{t,s} = 0 \quad \forall t \le T, s \le S, l \le L \tag{20}$$

$$-\overline{f}_l \le f_{t,l} \le \overline{f}_l \quad \forall t \le T, l \le L \tag{21}$$

$$-\pi \le \theta_{t,s} \le \pi \quad \forall t \le T, s \le S \backslash s : \text{reference bus} \tag{22}$$

$$\theta_{t,s_1} = 0 \quad \forall t \le T, s : \text{reference bus} \tag{23}$$

$$0 \le c_{t,w} \le wg_{t,w} + r_{t,w} \quad \forall t \le T, w \le W \tag{24}$$

$$0 \le LS_{t,s} \le D_{t,s} \quad \forall t \le T, s \le S \tag{25}$$

$$r_{t,w} = r_{t,w}^+ - r_{t,w}^- \quad \forall t \le T, w \le W \tag{26}$$

$$0 \le r_{t,w}^+ \le r_{t,w}^{\max} \quad \forall t \le T, w \le W \tag{27}$$

$$0 \le r_{t,w}^- \le r_{t,w}^{\max} \quad \forall t \le T, w \le W \tag{28}$$

$$\sum_{w=1}^{W} \frac{r_{t,w}^+ + r_{t,w}^-}{r_{t,w}^{\max}} \le \Gamma_t \quad \forall t \le T, w \le W \tag{29}$$

Objective function (1) minimizes total system operating cost under the worst wind realization. Constraints (2) and (3) represent binary logic to determine generator on/off, startup and shut down statuses. Constraints (4)–(6) model minimum up and down times, while constraints (7)–(9) calculate generators start-up costs. Constraints (10)–(13) determine generator outputs while respecting the minimum and maximum production limits, as well as ramping limits. Constraints (14)–(18) impose power and energy limits on storage operation and calculate state of charge. Constraints (19)–(25) represent transmission constraints of the DC power flow model. The uncertainty is modeled using constraints (26)–(29). The uncertain parameter in the model is wind deviation and it can be both positive (higher wind farm output than forecasted) or negative (lower wind farm output than forecasted), as indicated in (26). Maximum wind deviation is a known parameter and without the loss of generality in (27)–(28) we assume a symmetrical interval in which the wind deviation lies. Constraint (29) sets values of $r_{t,w}^+$ and $r_{t,w}^-$ depending on the robustness parameter Γ_t.

The model above is of max-min structure and cannot be solved directly. Since wind realization affects second stage variables, and is independent of the first stage, i.e., day-ahead variables, the problem can be rewritten using the min-max-min matrix form.

$$\min_x c_x^{\mathrm{T}} \cdot x \quad \max_r \quad \min_y \quad c_y^{\mathrm{T}} \cdot y \tag{30}$$

$$s.t. \quad Cy = -r - Bx \quad : \lambda \tag{31}$$

$$Dy \ge g - Ex - Fr \quad : \mu \tag{32}$$

$$s.t. \quad Hr \le h \tag{33}$$

$$s.t. \quad Ax \ge a \tag{34}$$

Equations (31)–(32) represent second stage cost and include constraints (10)–(25). The second-stage minimum cost is maximized over the uncertainty set described in equation (33) containing constraints (26)–(29). Equation (34) includes constraints (2)–(9) that model the day-ahead UC cost. By using the duality theory the inner min problem is transformed to max problem. The two maximization problems can be merged into a bilinear problem that is hard to solve and offers only a local optimum guarantee. Instead, by employing the KKT conditions to the inner maximization problem it is possible to convert the bilinear problem into a MILP that can be solved using an off-the-shelf solver [17]. The final model formulation is:

$$\min_x c_x^{\mathrm{T}} \cdot x \quad \max_{\lambda,\mu,r,\rho} -(Bx)^{\mathrm{T}}\lambda + (g - Ex)^{\mathrm{T}}\mu + h^{\mathrm{T}}\rho \tag{35}$$

$$s.t. \quad C^{\mathrm{T}}\lambda + D^{\mathrm{T}}\mu = c_y \tag{36}$$

$$\mu \ge 0 \tag{37}$$

$$0 \le \rho \quad \perp \quad h - Hr \ge 0 \tag{38}$$

$$H^{\mathrm{T}}\rho = -\lambda - F^{\mathrm{T}}\mu \tag{39}$$

$$s.t. \quad Ax \ge a \tag{40}$$

C. Solution algorithms

There are two solution algorithms to solve the obtained min-max problem. The first one is an iterative scheme based on cutting plane algorithm within a Benders' decomposition scheme. The steps of this algorithm are:

1) Set upper and lower bounds to a large enough number and initialize the iteration index $iter$ = 1.
2) Solve the relaxed master problem ($\min_x c_x^{\mathrm{T}} \cdot x + \beta$ subject to (40)). Fix a reasonable lower bound for β, i.e., lower than the expected objective value of the inner problem. Fix a feasible solution (x_1^*, β_1^*).
3) Solve the subproblem (the maximization problem) and update the upper bound. Add the Benders cut $\beta \ge -r_k \cdot \lambda_k + (g - F \cdot r_k) \cdot \mu_k - (\lambda_k \cdot B + \mu_k \cdot E) \cdot x$ to the relaxed master problem corresponding to the current solution.
4) Solve the master problem updated with Benders cuts and update the lower bound.
5) If the tolerance value is reached, then stop. Otherwise, update the iteration counter and go back to step 3.

Similarly to the Benders dual cutting plane algorithm, the problem can be solved using the C&CG algorithm that sig-

978-1-5386-2212-4/17/$31.00 ©2017 IEEE

TABLE I. STORAGE DATA

	$PC_m^{\max}$	$PD_m^{\max}$	$E_m^{\max}$
Storage at bus 116	50 MW	50 MW	300 MWh
Storage at bus 119	35 MW	35 MW	210 MWh
Storage at bus 121	100 MW	100 MW	600 MWh

TABLE II. MULTI Γ VALUES THROUGHOUT THE DAY

Hour	1	2	3	4	5	6	7	8	9	10	11	12
Γ	0	1	2	2	3	4	5	5	6	7	8	8
Hour	13	14	15	16	17	18	19	20	21	22	23	24
Γ	8	9	10	11	12	13	14	15	16	17	18	19

TABLE III. TOTAL SYSTEM OPERATING COSTS, $ (SUC – STARTUP COSTS; DC – DISPATCH COSTS)

	$\Gamma = 0$	$\Gamma = 8$	$\Gamma = 19$	Multi Γ
SUC	245,013	265,409	282,258	273,257
DC	916,650	949,449	1,073,280	952,986
Total	1,161,700	1,214,900	1,355,538	1,226,244

nificantly reduces the computing time. Instead of the Benders cut, several primal cuts are added:

$$\beta \geq c_y \cdot y_k \tag{41}$$

$$C \cdot y_k = -r_k - B \cdot x \tag{42}$$

$$D \cdot y_k = g - E \cdot x - F \cdot r_k \tag{43}$$

The equations (41)-(43) represent primal cutting planes in [14]. These cuts are affine in the primal recourse variables y_k and do not depend on dual variables. This allows us to use one Benders cut per vertex of the uncertainty set, as opposed to using one cut per joint feasibility set (r_k,λ,μ) which results in a smaller number of cuts.

III. CASE STUDY

The proposed model is tested on IEEE RTS-96 with additional 19 wind farms. All the test case data are available at [18]. Storage locations and capacities (shown in Table I) are chosen based on the technique proposed in [19]. Energy-to-power ratio is set to six, implying the installation of NaS battery technology [20].

Parameter Γ may range from 0 to 19, thus setting the number of wind farms that may deviate from their forecasted output. For $\Gamma = 0$, we obtain the deterministic case where all wind farms meet their expected output. On the other hand, $\Gamma = 19$ represents the full robust case when all wind farms deviate from their expected outputs. In the analysis we also show results for $\Gamma = 8$, which represents an average measure of protection. Additionally, since wind forecasts tend to deviate more further in the time horizon, we analyze the case with increasingly higher protection levels, i.e. Γ values, over time. Values of Γ over the course of the day are presented in Table II, while this case is referred to as "Multi Γ".

The results for four levels of conservatism are shown in Table III. The total system operating costs are 17% higher in case of the highest protection, i.e. $\Gamma = 19$ as opposed to the least conservative case where $\Gamma = 0$. Total operating costs do not increase linearly with Γ as for $\Gamma = 8$ the costs are only 4.5% higher than for the most optimistic case. These costs are similar to the ones for Multi Γ case. However, the structure of cost for Multi Γ is slightly different than for $\Gamma = 8$. Namely, the startup costs have higher share in the overall operating costs. This is the result of the Multi Γ case needing more generators on-line to satisfy the demand in the evening hours when the expected wind output is much lower due to high evenign Γ values.

Fig. 1 presents the effects of different levels of conservatism on conventional generators. Higher values of Γ incur higher conventional generation as the expected wind farm outputs are lower. The difference in certain hours is as high as 600 MW. The curve representing the Multi Γ (light) case starts very close to the optimistic case (dark curve), in hours 6–15 it is close to the $\Gamma = 8$ curve and in the evening hours it acts as the pessimistic case (dotted curve).

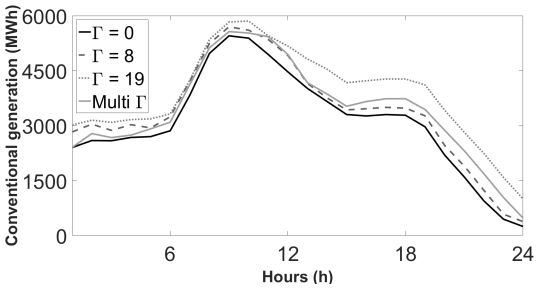

Fig. 1. Conventional generation.

Fig. 2 shows the levels of wind curtailment. Wind outputs in the evening are higher than early in the day and, consequently, the majority of wind curtailment occurs in the evening hours. Curtailment is highest for the optimistic case (dark curve). The Multi Γ curve is close to the pessimistic case (dotted curve)due to similar values of Γ in the evening hours.

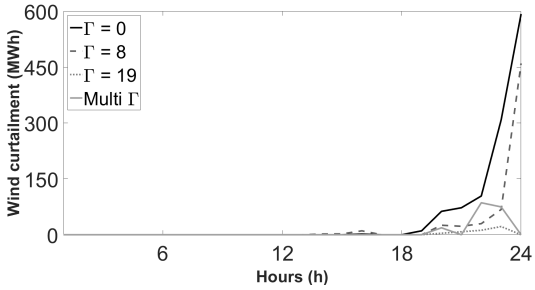

Fig. 3. Wind curtailment.

Fig. 3 shows the behaviour of the three storage units for different levels of protection. Generally, storage units slightly discharge in the first couple of hours and then start charging at full power rating until hour 6. After this, storage units start discharging until hour 13. At hour 20, the charging process occurs in order to reach the initial state of charge level imposed by constraint (18). In some cases, especially storage at bus

978-1-5386-2212-4/17/$31.00 ©2017 IEEE

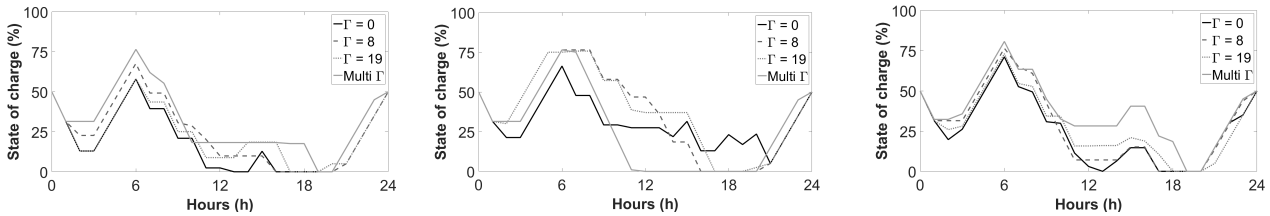

(a) Storage at bus 116 (b) Storage at bus 119 (c) Storage at bus 121

Fig. 2. Storage operation.

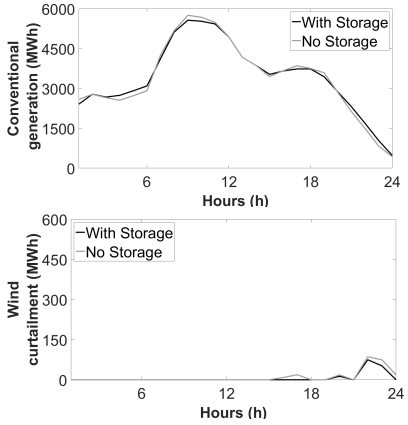

Fig. 4. Storage impact on conventional generation and wind curtailment for Multi Γ.

121, a small charging-discharging cycle occurs in the afternoon hours. The afternoon cycles are highest for $\Gamma = 19$.

The effects of storage in Multi Γ case are shown in Fig. 4. The daily peak of conventional generation that occurs at 9 am is reduced by 185 MW, while the conventional generation output is increased in early morning and late evening. Lower graph in Fig. 4 shows that the wind curtailment is reduced in presence of storage. This increased utilization of wind energy results in a reduction of overall operating cost from $1,271,331 to $1,226,244.

IV. Conclusions

This paper analyzes large-scale energy storage contribution to robust UC under different levels of protection. In the presented cases storage reduces total system operating costs by 2–4% and net load peak by 184 MW. This indicates the usefulness of storage and its compatibility with the robust UC framework.

Acknowledgement

This work was supported by the Croatian Science Foundation under project FENISG (grant no. 7766) and Croatian Transmission System Operator HOPS and Croatian Science Foundation under project SIREN (grant no. I-2583-2015).

References

[1] Y. V. Makarov, C. Loutan, M. Jian, and P. de Mello, "Operational impacts of wind generation on California Power Systems," *IEEE Trans. Power Syst.*, vol. 24, no. 2, pp. 1039–1050, May 2009.

[2] M. A. Ortega-Vazquez and D. S. Kirschen, "Optimizing the spinning reserve requirements using a cost/benefit analysis,"*IEEE Trans. Power Syst.*, vol. 22, no. 1, pp. 24–33, Feb. 2007.

[3] J. M. Arroyo and F. D. Galiana, "Energy and reserve pricing in security and network-constrained electricity markets,"*IEEE Trans. Power Syst.*, vol. 20, no. 2, pp. 634–643, May 2005.

[4] J. Wang, M. Shahidehpour, and Z. Li, "Security-constrained unit commitment with volatile wind power generation," *IEEE Trans. Power Syst.*, vol. 23, no. 3, pp. 1319–1327, Aug. 2008.

[5] S. Takriti, J. R. Birge, and E. Long, "A stochastic model for the unit commitment problem," *IEEE Trans. Power Syst.*, vol. 11, no. 3, pp. 1497–1508, Aug. 1996.

[6] P. Carpentier, G. Cohen, J. C. Culioli, and A. Renaud, "Stochastic optimization of unit commitment: A new decomposition framework," *IEEE Trans. Power Syst.*, vol. 11, no.2, pp. 1067–1073, Aug. 1996.

[7] H. Pandžić, Y. Dvorkin, T. Qiu, Y. Wang, and D. S. Kirschen, "Toward Cost-Efficient and Reliable Unit Commitment Under Uncertainty," *IEEE Trans. Power Syst.*, vol. 31, no. 2, pp. 970–982, Mar. 2016.

[8] Y. Wang, Q. Xia, and C. Kang, "Unit commitment with volatile node injections by using interval optimization," *IEEE Trans. Power Syst.*, vol. 26, no. 3, pp. 1705–1713, Aug. 2011

[9] A. Ben-Tal, L. El Ghaoui, and A. Nemirovski, "Robust Optimization," Princeton University Press Princeton and Oxford, 2009.

[10] DOE Global Energy Storage Database [Online]. Available at: www.energystorageexchange.org/projects

[11] M. G. Rasmussen, G. B. Andersen, and M. Greiner, "Storage and Balancing Synergies in a Fully or Highly Renewable Pan-European Power System," *Energy Policy*, vol. 51, no. 2, pp. 642–651, 2012.

[12] D. Bertsimas, E. Litvinov, X. A. Sun, J. Zhao, and T. Zheng, "Adaptive Robust Optimization for the Security Constrained Unit Commitment Problem," *IEEE Trans. Power Syst.*, vol. 28, no. 1, pp. 52–63, Feb. 2013.

[13] L. Zhao and B. Zeng, "Robust Unit Commitment Problem with Demand Response and Wind Energy," in Proc. PES General Meeting, 22-26 July 2012.

[14] B. Zeng, "Solving Two-stage Robust Optimization Problems by a Constraint-an-Column Generation Method." [Online]. Available at: http://www.optimization-online.org/DB_FILE/2011/06/3065.pdf

[15] R. Jiang, M. Zhang, G. Li, and Y. Guan, "Two-Stage network constrained robust unit commitment problem," *European Journal of Operational Research*, vol. 234, no. 3, Feb. 2014.

[16] R. Jiang, J. Wang, and Y. Guan, "Robust Unit Commitment with Wind Power and Pumped Storage Hydro," *IEEE Trans. Power Syst.*, vol. 27, no. 2, May 2012.

[17] S. A. Gabriel, A. J. Conejo, J. D. Fuller, B. F. Hobbs, and C. Ruiz. "Complementarity Modeling in Energy Markets", Springer, 2013.

[18] H. Pandžić, Y. Dvorkin, T. Qiu, Y. Wang, and D. Kirschen, Unit Commitment under Uncertainty GAMS Models, Library of the Renewable Energy Analysis Lab (REAL), University of Washington, Seattle, USA. [Online]. Available at: www.ee.washington.edu/research/real/gamscode.html

[19] H. Pandžić, Y. Wang, T. Qiu, Y. Dvorkin, and D. Kirschen, "Near-Optimal Method for Siting and Sizing of Distributed Storage in a Transmission Network," *IEEE Trans. Power Syst.*, vol. 30, no. 5, Sept. 2015.

[20] M. Kintner-Meyer et al., "Energy Storage for Power Systems Applications: A Regional Assessment for the Northwest Power Pool (NWPP)," [Online], Available at: energyenvironment.pnnl.gov/ei/pdf/NWPP%20report.pdf